PHYSICAL REVIEW B **89**, 041109(R) (2014)

Nonmagnetic ground state of PuO_2

A. B. Shick,[1] J. Kolorenč,[1] L. Havela,[2] T. Gouder,[3] and R. Caciuffo[3]
[1]*Institute of Physics, ASCR, Na Slovance 2, CZ-18221 Prague, Czech Republic*
[2]*Department of Condensed Matter Physics, Charles University, Ke Karlovu 5, CZ-12116 Prague, Czech Republic*
[3]*European Commission, Joint Research Centre, Institute for Transuranium Elements, Postfach 2340, D-76125 Karlsruhe, Germany*
(Received 30 September 2013; published 30 January 2014)

The correlated band theory implemented as a combination of the local density approximation with the exact diagonalization of the Anderson impurity model is applied to PuO_2. We obtain an insulating electronic structure consistent with the experimental photoemission spectra. The calculations yield a band gap of 1.8 eV and a nonmagnetic singlet ground state that is characterized by a noninteger filling of the plutonium f shell ($n_f \approx 4.5$). Due to sizable hybridization of the f shell with the p states of oxygen, the ground state is more complex than the four-electron Russell-Saunders $^5I_4$ manifold split by the crystal field. The inclusion of hybridization improves the agreement between the theory and experiment for the magnetic susceptibility.

DOI: 10.1103/PhysRevB.89.041109 PACS number(s): 71.20.Nr, 71.27.+a, 75.40.Cx

In order to fully utilize the potential of nuclear power, maintaining at a minimum level the risks associated with the deployment of this technology, it is necessary to solve the problems of characterization, treatment, and disposal of high-level nuclear waste. On a time scale of several hundred years, the waste from the open fuel cycle will predominantly contain Pu and minor actinides. Their geological disposal requires a waste handling technology of exceptional durability, with a highly reduced risk of accidental events. That is why comprehensive knowledge of the physical and chemical properties of actinide-based oxides (AnO_2, An = Th, U, Np, Pu, Am, Cm), which constitute the main part of long-lived nuclear waste, remains a key topic of condensed matter theory.

PuO_2 crystallizes in the well-known CaF_2 fluorite structure, with eight-coordinated Pu and four-coordinated O. For divalent oxygen, the stoichiometry implies a $5f^4$ configuration for Pu^{4+}. PuO_2 is an insulator with a band gap of 1.8 eV [1] and a temperature independent magnetic susceptibility [2]. Recent nuclear magnetic resonance studies suggest a vanishing local magnetic moment in this compound [3].

While experimentally the absence of magnetism is clear, its theoretical understanding remains controversial. The crystal-field (CF) theory [4] explains this nonmagnetic behavior in terms of a Γ_1 nonmagnetic singlet ground state, which results from the CF splitting of the $J = 4$ ($^5I_4$) manifold. The CF picture is consistent with the inelastic neutron scattering spectra [5] observing a single peak, corresponding to the $\Gamma_1 \rightarrow \Gamma_4$ transition, at an energy of 123 meV. However, the measured value of the magnetic susceptibility $\chi(T)$ is only 50% of what one would expect from the Van Vleck coupling, and its temperature dependence is weaker than the one predicted by the CF model. The average value of χ in the temperature interval up to about 1000 K can be reproduced if the Γ_4 level is taken at 284 meV and not at 123 meV as observed. Several alternative mechanisms that could decrease the magnitude of the susceptibility while keeping the $\Gamma_1 \rightarrow \Gamma_4$ gap at 123 meV have been proposed. One of them is an effective reduction of the orbital moment by Pu f–O p covalency [5], and another involves a negative contribution to χ due to an antiferromagnetic Weiss exchange field (see, e.g., Ref. [4] and references therein). Nevertheless, the temperature independence of the susceptibility is not explained in these models.

The band-theoretical modeling of the electronic, structural, and magnetic character of actinide materials and their $5f$ states is very difficult. The conventional density functional theory (DFT) in the local spin density (LSDA) and generalized gradient (GGA) approximations falls short in explaining the insulating character of PuO_2 as well as other actinide oxides [6]. It is now widely accepted that in order to successfully model the actinide materials, the electron correlations need to be accounted for beyond the conventional DFT. One of the possibilities is provided by the so-called hybrid exchange-correlation functionals [6]. Unfortunately, these calculations yield an antiferromagnetic ground state, in disagreement with experiments.

Contrary to the hybrid functionals, the so-called LSDA+Hubbard U (LDA+U) functional can produce an insulating nonmagnetic solution for PuO_2 [7,8]. However, this solution is not the minimum energy state, and ferromagnetic and antiferromagnetic spin-polarized LDA+U solutions are lower in energy. Thus the Pu atom magnetic moment is not quenched, and the experimentally observed temperature independent magnetic susceptibility of PuO_2 is not explained by LDA+U calculations.

In this Rapid Communication, we extend the LDA+U method by making use of a combination of LDA with the exact diagonalization of the Anderson impurity model (ED) [9,10]. We show that the LDA+ED calculations with the Coulomb $U = 6.5$ eV and the exchange $J = 0.5$ eV yield a nonmagnetic singlet ground state with an f-shell occupation $n_f \approx 4.5$ at the Pu atoms. The noninteger filling of the f shell is a consequence of a hybridization with the p states of oxygen. In contrast, the ionic bonding with formally divalent oxygen assumed in the crystal-field theory would require an integer filling ($n_f = 4$). The ground state is found to be separated from the first excited triplet state by 126 meV. The LDA+ED electronic structure is insulating with a band gap of 1.8 eV and the calculated density of states (DOS) is consistent with the experimental results of photoelectron spectroscopy (PES).

The starting point of our approach is the multiband Hubbard Hamiltonian $H = H^0 + H^{\text{int}}$, where H^0 is the one-particle

Hamiltonian found from *ab initio* electronic structure calculations of a periodic crystal; $H^{\rm int}$ is the on-site Coulomb interaction [11] describing the $5f$-electron correlation. We use the LDA for the electron interactions in other than f shells. The effects of the interaction Hamiltonian $H^{\rm int}$ on the electronic structure are described with the aid of an auxiliary impurity model describing the complete seven-orbital $5f$ shell. This multiorbital impurity model includes the full spherically symmetric Coulomb interaction, the spin-orbit coupling (SOC), and the crystal field. The corresponding Hamiltonian can be written as [12]

$$\begin{aligned} H_{\rm imp} = & \sum_{\substack{kmm'\\ \sigma\sigma'}} [\epsilon^k]^{\sigma\ \sigma'}_{mm'} b^\dagger_{km\sigma} b_{km'\sigma'} + \sum_{m\sigma} \epsilon_f f^\dagger_{m\sigma} f_{m\sigma} \\ & + \sum_{mm'\sigma\sigma'} [\xi \mathbf{l}\cdot\mathbf{s} + \Delta_{\rm CF}]^{\sigma\ \sigma'}_{mm'} f^\dagger_{m\sigma} f_{m'\sigma'} \\ & + \sum_{\substack{kmm'\\ \sigma\sigma'}} ([V^k]^{\sigma\ \sigma'}_{mm'} f^\dagger_{m\sigma} b_{km'\sigma'} + \text{H.c.}) \\ & + \frac{1}{2} \sum_{\substack{mm'm''\\ m'''\sigma\sigma'}} U_{mm'm''m'''} f^\dagger_{m\sigma} f^\dagger_{m'\sigma'} f_{m'''\sigma'} f_{m''\sigma}, \end{aligned} \quad (1)$$

where $f^\dagger_{m\sigma}$ creates an electron in the $5f$ shell and $b^\dagger_{m\sigma}$ creates an electron in the "bath" that consists of those host-band states that hybridize with the impurity $5f$ shell. The energy position ϵ_f of the impurity level and the bath energies ϵ^k are measured from the chemical potential μ. The parameter ξ specifies the strength of the SOC and $\Delta_{\rm CF}$ is the crystal-field potential at the impurity. The parameter matrices V^k describe the hybridization between the $5f$ states and the bath orbitals at energy ϵ^k.

The band Lanczos method [9] is employed to find the lowest-lying eigenstates of the many-body Hamiltonian $H_{\rm imp}$ and to calculate the one-particle Green's function $[G_{\rm imp}(z)]^{\sigma\ \sigma'}_{mm'}$ in the subspace of the f orbitals at low temperature ($k_{\rm B}T = \beta^{-1} = 1/500$ eV). Then, with the aid of the local Green's function $G_{\rm imp}(z)$, we evaluate the occupation matrix $n_{\gamma_1\gamma_2} = \frac{1}{\beta}\sum_\omega [G_{\rm imp}(i\omega)]_{\gamma_1\gamma_2} + \frac{1}{2}\delta_{\gamma_1\gamma_2}$, where the composite index $\gamma \equiv (lm\sigma)$ labels the spinorbitals.

The matrix $n_{\gamma_1\gamma_2}$ is used to construct an effective LDA+U potential V_U, which is inserted into Kohn-Sham-like equations [13]:

$$[-\nabla^2 + V_{\rm LDA}(\mathbf{r}) + V_U + \xi(\mathbf{l}\cdot\mathbf{s})]\Phi^b_{\mathbf{k}}(\mathbf{r}) = \epsilon^b_{\mathbf{k}}\Phi^b_{\mathbf{k}}(\mathbf{r}). \quad (2)$$

These equations are iteratively solved until self-consistency over the charge density is reached. In each iteration a new value of the $5f$-shell occupation is obtained from the solution of Eq. (2), and the next iteration is started by solving Eq. (1) for the updated $5f$-shell filling. The self-consistent procedure was repeated until the convergence of the $5f$-manifold occupation n_f was better than 0.02.

Once the self-consistency is reached, the eigenvalues $\epsilon_{\mathbf{k}}$ of Eq. (2) are corrected to account for the self-energy $\Sigma(\epsilon)$ of the impurity model Eq. (1) (see the Supplemental Material for additional details [14]). We make use of the first-order perturbation theory to write an eigenvalue correction,

$$\mathrm{E}^n_{\mathbf{k}} = \epsilon^n_{\mathbf{k}} + \mathrm{Re}\left\langle \Phi^n_{\mathbf{k}} \middle| \Sigma\left(\epsilon^n_{\mathbf{k}}\right) - V_U \middle| \Phi^n_{\mathbf{k}} \right\rangle. \quad (3)$$

The SOC parameter $\xi = 0.30$ eV for PuO_2 was determined from LDA calculations. CF effects were described by the crystal-field potential for the cubically coordinated f shell,

$$\begin{aligned} \Delta_{\rm CF} = & \frac{16\sqrt{\pi}}{3} V_4 \left(Y^0_4 + \sqrt{\frac{10}{7}}\,\mathrm{Re}\, Y^4_4 \right) \\ & + 32\sqrt{\frac{\pi}{13}} V_6 \left(Y^0_6 - \sqrt{14}\,\mathrm{Re}\, Y^4_6 \right), \end{aligned} \quad (4)$$

where V_4 and V_6 were chosen as external parameters. In the actual calculations, we used the values $V_4 = -0.151$ eV and $V_6 = 0.031$ eV deduced from experimental data in Ref. [5], and close to the estimate given in Ref. [15]. The CF parameters could be also calculated using *ab initio* approaches [16], and we plan to do so in the future.

In order to specify the bath parameters, we assume that LDA represents the noninteracting model for PuO_2, and associate with it the solution of Eq. (1) without the last Coulomb-interaction term. Moreover, we assume that the first and fourth terms in Eq. (1) are diagonal in a $\{j, j_z\}$ representation. Next, we obtain $V^{j=5/2,7/2}_{k=1}$ and $\epsilon^{5/2,7/2}_{k=1}$ from the LDA hybridization function $\Delta(\epsilon) = -\frac{1}{\pi N_f}\,\mathrm{Im\,Tr}[G^{-1}(\epsilon + i\delta)]$, where $N_f = 6$ for $j = 5/2$, $N_f = 8$ for $j = 7/2$, and G is the LDA Green's function. The hybridization function $\Delta(\epsilon)$ is shown in Fig. 1 together with the O-p- and Pu-f-projected LDA densities of states. As follows from Fig. 1, the most essential hybridization occurs in the energy region of the O-p states. We set $\epsilon^{5/2,7/2}_{k=1}$ to the -2.92 eV peak position of $\Delta(\epsilon)$, and obtain $V^{j=5/2}_{k=1} = 1.46$ eV and $V^{j=7/2}_{k=1} = 1.62$ eV at the peak position of $\Delta(\epsilon)$.

The Slater integral F_0 (Coulomb U) is regarded as an adjustable parameter; calculations have been performed for $U = 4.5$, 5.5, and 6.5 eV, within the range commonly considered in the literature. For the other Slater integrals we have used the values $F_2 = 5.96$ eV, $F_4 = 3.982$ eV, and $F_6 = 2.946$ eV

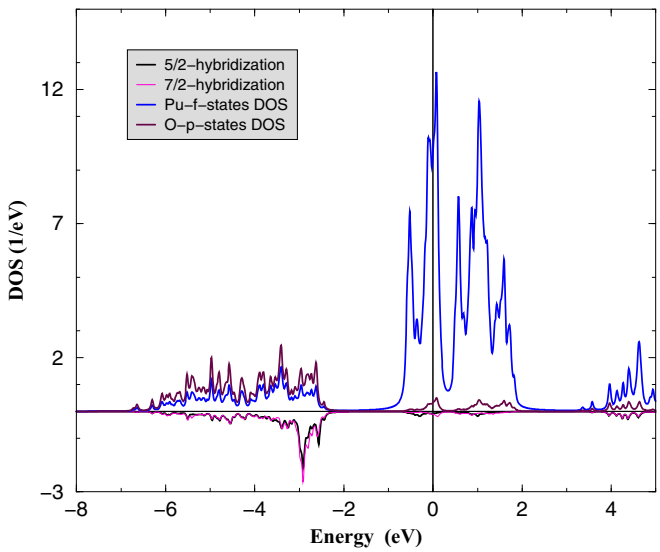

FIG. 1. (Color online) The O-p- and Pu-f-projected DOS, and the hybridization function $\Delta(\epsilon)$ (the negative y-axis scale, eV).

that have been obtained by scaling the atomic Hartree-Fock results [17] to approximately 60% to account for configuration interactions and screening effects. The screened integrals correspond to the Hund's exchange $J = 0.5$ eV, which is in the ballpark of the values used in the LDA+U [6] and LDA+DMFT (dynamical mean field theory) [18] calculations. For the double-counting term (included in the potential V_U) we have adopted the fully localized (or atomiclike) limit (FLL) $V_{\rm dc} = U(n_f - 1/2) - J(n_f - 1)/2$.

In the calculations we used an in-house implementation [19,20] of the full-potential linearized augmented plane wave (FP-LAPW) method that includes both scalar-relativistic and spin-orbit coupling effects. The calculations were carried out assuming a paramagnetic state and a cubic fluorite crystal structure. We set the radius of the Pu atomic sphere to 2.65 a.u. and the O atomic sphere to 1.70 a.u. The parameter $R_{\rm Pu} \times K_{\rm max} = 9.3$ determined the basis set size, and the Brillouin zone was sampled with 4000 k points.

Now we turn to the results of LDA+ED calculations. For the set of $U = 4.5$ eV and $J = 0.5$ eV, solving self-consistently Eqs. (1) and (2), we obtain the f occupation $n_f = 4.58$ close to conventional LDA+U with the same U and J ($n_f = 4.56$) as well as to the occupation deduced from the $4f$ x-ray photoemission spectroscopy (XPS, $n_f = 4.65$ [21]). After applying the eigenvalue correction Eq. (3), we do not obtain an insulating state. Once the Coulomb U is increased, say, to 5.5 eV, the PuO_2 becomes an insulator with a band gap of 1.4 eV (see the Supplemental Material, Table S2 [14]). For the Coulomb $U = 6.5$ eV (and $J = 0.5$ eV), we obtain an insulating solution with a band gap of 1.8 eV. When the value of $J = 0.6$ eV is used, the band gap value is slightly reduced to 1.6 eV. The corresponding total density of states (TDOS), the Pu atom f-state, and the O atom p-state partial DOS are shown in Fig. 2.

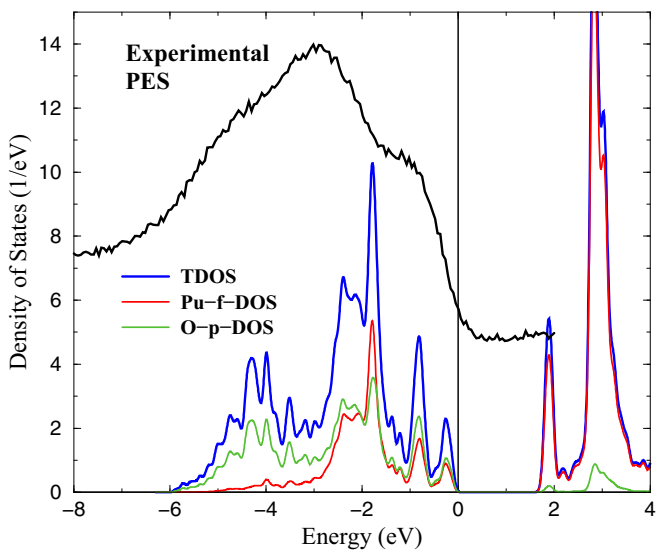

FIG. 2. (Color online) The total, O-p-, and Pu-f-projected DOS from LDA+ED calculations with $U = 6.5$ eV, $J = 0.5$ eV, together with the experimental PES (spectrum, recorded with the He II excitation, photon energy 40.81 eV). Note that the PES spectrum is adjusted to match the upper edge with the zero energy.

The experimental PES [22–24] (see Fig. 2; note the horizontal shift of the data) is usually obtained on PuO_2 films prepared by reactive sputter deposition from an α-Pu target in an Ar/O_2 plasma. The O_2 partial pressure was adjusted to obtain the correct stoichiometry. Peaks are observed at 2 and 4 eV binding energy (BE), with a shoulder at 6 eV BE. The orbital parentage of the peaks can be deduced by comparing the intensities obtained for He I and He II radiation (photon energy equal to 21.22 and 40.81 eV, respectively). The He I spectrum is dominated by the O-p emission, whereas for He II the Pu-f and O-p contributions are comparable. It is concluded that the 2 eV BE peak stems from the Pu-f states. This peak is usually considered as an indication of the f^4 nominal configuration, corresponding to the Pu^{4+} oxidation state. The next (4 eV BE) peak is more intense and broad. The He II and He I spectral difference indicates a substantial O-p character of this peak. The shoulder at 6 eV BE is associated mostly with the O-p states. As the calculations associate the upper edge of the conduction band with zero binding energy, the experimental spectrum was shifted for the sake of comparison towards the zero energy as well.

The LDA+ED DOS shown in Fig. 2 has a peak with the mixed Pu-f and O-p characters at $\approx$0.8 eV below the E_F (with an additional smaller satellite closer to the E_F). Another broad peak at ≈ -2 eV has more intensity (for both f and p states), and there is a broad, dominantly O-p character, shoulder between -3 and -6 eV. Thus, if we consider the difference in the peak positions, they correspond reasonably to the experiment. Their absolute values differ from the experimental BE [22–24] by $\approx$1–1.5 eV. The reason is that in PES experiments the Fermi level falls in the middle of the band gap, while the upper edge of the conduction band defines the Fermi level in the calculations. Both the experiment and calculations suggest a mixture of f^4 and f^5 configurations in the ground state due to Pu-5f and O-2p hybridization.

Now we turn to the salient theme of our investigation, the ground state of the impurity model Eq. (1). This ground state is a singlet formed by the 5f shell and the bath with occupation numbers $\langle n_f \rangle = 4.52$ in the f shell and $\langle n_{\rm bath} \rangle = 13.48$ in the bath states. Since the ground state is a singlet, any magnetic or multipolar degree of freedom is frozen when the temperature is well below the gap between the ground state and excited states. The calculated energy difference between this ground state and the first excited states (triplet) is 126 meV, very close to the experimental value of 123 meV, which was observed in the inelastic neutron scattering spectra [5]. Neither the ground state nor the excited states are exact crystal-field states since they involve the p states of oxygen.

Analogously to the crystal-field theory, the impurity model can be used to estimate the magnetic susceptibility and its temperature dependence by adding the action of an external magnetic field B_z to Eq. (1),

$$\hat{H}_B = -\sum_{m\sigma} \mu_{\rm B} B_z \left([\hat{l}_z + 2\hat{s}_z]^{\sigma}_{mm} \, \hat{f}^{\dagger}_{m\sigma} \hat{f}_{m\sigma} + [2\hat{s}_z]^{\sigma}_{mm} \, \hat{b}^{\dagger}_{m\sigma} \hat{b}_{m\sigma} \right) . \tag{5}$$

The bath originates from the LDA oxygen bands and hence the magnetic field couples only to the spin degrees of freedom in this part of the impurity model. When the

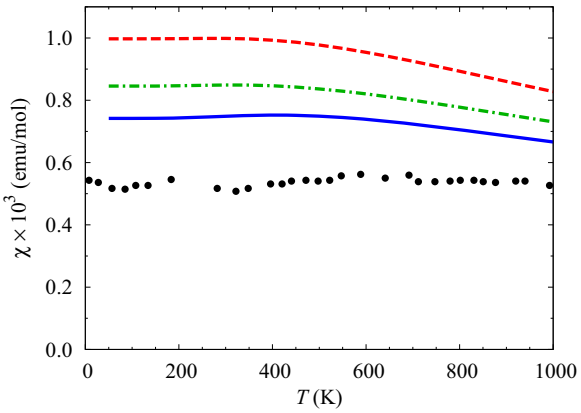

FIG. 3. (Color online) Temperature dependence of the molar magnetic susceptibility calculated in the crystal-field theory ($\chi_{\rm CF}$, red dashed line) and in the impurity model ($\chi_{\rm imp}$, green dotted-dashed line) for $U = 6.5$ eV and $J = 0.5$ eV. The blue solid line shows $\chi_{\rm imp}$ with the exchange enlarged to $J = 0.6$ eV. The black dots are the experimental data from Ref. [2].

magnetic field is weak and the linear-response regime applies, we can get the molar magnetic susceptibility from the induced f-shell magnetic moment $m_z(T) = \mu_{\rm B}\langle \hat{l}_z + 2\hat{s}_z\rangle$ as $\chi_{\rm imp}(T) = \mu_0 N_{\rm A} m_z(T)/B_z$, where μ_0 stands for the vacuum permeability.

The susceptibility $\chi_{\rm imp}$ calculated for $U = 6.5$ eV and $J = 0.5$ eV is shown in Fig. 3 in comparison with the susceptibility $\chi_{\rm CF}$ from the crystal-field theory, that is, from Eq. (1) without the bath. The hybridization of the f orbitals with the ligand states reduces the magnitude of the susceptibility as well as its temperature dependence and hence brings the theory closer to the experimental findings [2]. Here we in fact estimate the magnitude of the covalency effects discussed in Ref. [5]. Furthermore, it turns out that $\chi_{\rm imp}$ is sensitive to the exchange parameter J, whereas it is essentially independent on U. With $J = 0.6$ eV, the temperature dependence is further suppressed and the magnitude of $\chi_{\rm imp}$ is only about 35% larger than the experiment (see Fig. 3 and compare to a nearly 100% overestimation of the crystal-field theory alone). The $\Gamma_1 \to \Gamma_4$ gap practically does not depend on J. The reduced temperature dependence is a result of the cancellation of temperature-dependent parts of the induced moments $\mu_{\rm B}\langle \hat{l}_z\rangle$ and $\mu_{\rm B}\langle 2\hat{s}_z\rangle$ that both deviate from a constant above 300 K due to the increasing population of the excited-state triplet Γ_4. See the Supplemental Material for an illustration and for additional details of the J dependence of $\chi_{\rm imp}$ [14].

In summary, by making use of the LDA+ED calculations with $U = 6.5$ eV and $J = 0.5$ eV, we obtain a nonmagnetic singlet ground state with $n_f \approx 4.5$ for Pu atoms in PuO_2. The LDA+ED yields an insulating electronic structure consistent with the experimental photoelectron spectra. The band gap is found to be 1.8 eV. The energy difference between the ground state and the first excited triplet state is 126 meV, in agreement with the experimental inelastic neutron scattering spectra. The calculated singlet ground state and the consequent nonmagnetic behavior have a lot in common with the outcome of the crystal-field theory; the significant improvement is that LDA+ED achieves these features for a realistic noninteger occupation of the Pu f orbitals. We emphasize that we did not adjust the model parameters to fit the experimental findings. Instead, we investigated the dependence of physically observable quantities on the choice of these parameters.

Financial support from the Czech Republic Grant No. GACR P204/10/0330 is acknowledged.

[1] C. E. McNeilly, J. Nucl. Mater. **11**, 53 (1964).
[2] G. Raphael and R. Lallement, Solid State Commun. **6**, 383 (1968).
[3] H. Yasuoka *et al.*, Science **336**, 901 (2012).
[4] P. Santini *et al.*, Rev. Mod. Phys. **81**, 807 (2009).
[5] S. Kern, R. A. Robinson, H. Nakotte, G. H. Lander, B. Cort, P. Watson, and F. A. Vigil, Phys. Rev. B **59**, 104 (1999).
[6] X.-D. Wen *et al.*, Chem. Rev. **113**, 1063 (2013).
[7] H. Nakamura, M. Machida, and M. Kato, Phys. Rev. B **82**, 155131 (2010).
[8] M.-T. Suzuki, N. Magnani, and P. M. Oppeneer, Phys. Rev. B **88**, 195146 (2013).
[9] J. Kolorenc, A. I. Poteryaev, and A. I. Lichtenstein, Phys. Rev. B **85**, 235136 (2012).
[10] A. B. Shick, J. Kolorenc, J. Rusz, P. M. Oppeneer, A. I. Lichtenstein, M. I. Katsnelson, and R. Caciuffo, Phys. Rev. B **87**, 020505 (2013).
[11] A. I. Lichtenstein and M. I. Katsnelson, Phys. Rev. B **57**, 6884 (1998).
[12] A. Hewson, *The Kondo Problem to Heavy Fermions* (Cambridge University Press, Cambridge, UK, 1993).
[13] A. B. Shick, J. Kolorenc, A. I. Lichtenstein, and L. Havela, Phys. Rev. B **80**, 085106 (2009).
[14] See Supplemental Material at http://link.aps.org/supplemental/10.1103/PhysRevB.89.041109 for the details of the LDA+U, the Anderson impurity model, and magnetic susceptibility calculations.
[15] N. Magnani, P. Santini, G. Amoretti, and R. Caciuffo, Phys. Rev. B **71**, 054405 (2005).
[16] P. Novak, K. Knizek, and J. Kunes, Phys. Rev. B **87**, 205139 (2013).
[17] K. Moore and G. van der Laan, Rev. Mod. Phys. **81**, 235 (2009).
[18] Q. Yin, A. Kutepov, K. Haule, G. Kotliar, S. Y. Savrasov, and W. E. Pickett, Phys. Rev. B **84**, 195111 (2011).
[19] A. B. Shick, A. I. Liechtenstein, and W. E. Pickett, Phys. Rev. B **60**, 10763 (1999).
[20] A. B. Shick and W. E. Pickett, Phys. Rev. Lett. **86**, 300 (2001).
[21] A. Kotani and T. Yamazaki, Prog. Theor. Phys. Suppl. **108**, 117 (1992).
[22] M. T. Butterfield *et al.*, Surf. Sci. **571**, 74 (2004).
[23] T. Gouder, A. Seibert, L. Havela, and J. Rebizant, Surf. Sci. **601**, L77 (2007).
[24] T. Gouder, A. Shick, and F. Huber, Top. Catal. **56**, 1112 (2013).